KJVR
Korean Journal of Veterinary Research

Original Article

pISSN 2466-1384 · eISSN 2466-1392
Korean J Vet Res 2021;61(3):e25
https://doi.org/10.14405/kjvr.2021.61.e25

*Corresponding author:
Seda Karabulut
Department of Histology and Embryology, School of Medicine, Istanbul Medipol University, Göztepe Distinct, Atatürk Street, No:40/16, Istanbul 34810, Turkey
Tel: +90-216-681-51-00
Fax: +90-212-521-23-77
E-mail: sedakarabulut@medipol.edu.tr

ORCID:
https://orcid.org/0000-0003-3302-5004

Conflict of interest:
The authors declare no conflict of interest.

Received: April 30, 2021
Revised: June 15, 2021
Accepted: June 17, 2021

Detailed morphological analysis of axolotl sperm

İlknur Keskin[1,2], Duygu Gürsoy Gürgen[1,2], Didem Avinca[1,2], Ekrem Musa Özdemir[2,3], Suat Utku Keskin[4], Seda Karabulut[1,2,*]

[1]Department of Histology and Embryology, School of Medicine, Istanbul Medipol University, Istanbul 34810, Turkey
[2]Research Institute for Health Sciences and Technologies (SABITA), Istanbul Medipol University, Istanbul 34810, Turkey
[3]Medical Research Center (MEDİTAM), Research Institute for Health Sciences and Technologies (SABITA), Istanbul Medipol University, Istanbul 34810, Turkey
[4]Robert College, Istanbul 34345, Turkey

The axolotl has extraordinary regeneration capacity compared to other vertebrates. This remarkable potential has been attributed to its life-long neoteny, characterized by the exhibition of embryonic characteristics at the adult stage. A recent study provided a detailed morphological analysis of the sperm morphology of the *Ambystoma mexicanum* using routine and detailed histological techniques. The primary purpose of the present study is to describe a simple and inexpensive method for evaluating the morphology of axolotl sperm. In this study, spermatophore structures were collected and spread on slides and air-dried. The slides were stained with periodic acid Schiff, toluidine blue, Masson's trichrome, Giemsa, Spermac, and Diff-Quik dye for a morphological examination. The slides were coated with gold/palladium for a scanning electron microscopy examination. The sperm of the axolotl consisted of an elongated head, a neck, and a flagellum covered with an undulating membrane. The lengths of the midpiece, tail, and head were 8.575 μm, 356.544 μm, and 103.661 μm, respectively. In the flagellum part, the wavy membrane structure, whose function has not been explained, surrounds the tail. The data obtained from this study will constitute an important step in designing future research on the reproductive and regeneration capacity of the axolotl.

Keywords: *Ambystoma mexicanum*; spermatozoa; histology

Introduction

Ambystoma mexicanum (axolotl), also known as the Mexican salamander, is an endemic amphibian species whose natural habitat is Chalco in Mexico and the Xochimilco Valley, belonging to the family Ambystomatidae. There are more than 30 salamander species in the *Ambystoma* genus.

The axolotl can regenerate their internal organs, limbs, spinal cord, tail, and brain [1]. It has extraordinary regeneration capacity in proportion to other vertebrates [2].

This remarkable regenerative potential has been attributed to the life-long neoteny of the axolotl, which is characterized by the exhibition of embryonic characteristics at the adult stage. Unlike most amphibians, axolotls never metamorphose into lung-breathing, terrestrial adults.

The male lays a sack of male jelly, a small white capsule full of sperm known as a spermatophore. The spermatophore is a characteristic structure of most male uro-

deles that have internal fertilization, more than 90%. The female has one or more sacks on her cloaca [3]. Spermatophores are picked up by the female cloaca, where the sperm are released and wait in the spermatheca at the exit of the oviduct until fertilization [4]. The sperm inside the female can fertilize the eggs. Females align the eggs to aquatic plants when fertilization is completed [5]. She will eventually begin laying eggs, which can take hours or even days to start. She may lay between 100 and 1,000 eggs at this time. The eggs are soft and covered in a slime that keeps them grouped. The eggs firm up as the larva grows. After a few weeks, many new larval axolotls are produced. Axolotls undergo this courtship once a year, particularly from March to June. Female axolotl attaches her 100 to 300 jelly-coated eggs to aquatic plants or rocks. Approximately 10 to 14 days later, the eggs hatch. Axolotls become sexually mature after approximately 1 year.

The studies are concentrated in the field of the regeneration ability and evolutionary biology of the axolotl. Research on the reproductive biology and gametes of the axolotl is very limited.

This paper reports a detailed morphological analysis of the sperm cells of *A. mexicanum* using several microscopic techniques. The data obtained will constitute an important step for future studies on the reproduction and regeneration capacity of *A. mexicanum*.

Materials and Methods

Animal care and sample collection

The EU Directive 2010/63/EU for animal experiments guidelines were followed. Animal care conditions and experiments were authorized with the approval number 38828770-604.01.01-E.32248 by the local ethics committee of the Istanbul Medipol University. The animals were maintained in individual aquaria within a Holtfreter's solution at 18°C. This research did not receive any specific grant from funding agencies in the public, commercial, or not-for-profit sectors.

In the present study, the spermatophore (sperm packets) structures that the sexually mature axolotl left in the water tank were collected. If spermatophore structures were not found, the protocol developed by Mansour et al. [6] was used. This protocol was developed to collect *A. mexicanum* gametes. Sperm was collected by applying an abdominal massage to three animals (n = 3) under 0.1% benzocaine (Cat. No. E10521; Sigma-Aldrich, USA) anesthesia and the animals were not harmed. Samples collected from each animal were spread over 21 slides (3 repeats for each method) and air-dried. The remaining sperm were stored under suitable conditions for the other examinations. Except for the Diff-Quik staining protocol, the specimens were fixed in 4% paraformaldehyde (SZBF1870V; Sigma-Aldrich) and washed with distilled water. For the morphological examination, the slides were stained with periodic acid Schiff (PAS), toluidine blue, Masson's trichrome, Giemsa, Spermac, and Diff-Quik dye according to manufacturer's protocol and visualized by microscopy (Nikon Eclipse; Nikon Instruments Inc., USA) using a Nikon DS-Fi2-U3 Digital Camera and its image analysis software system. Each part of the sperm cell was measured using the Image J program (US National Institutes of Health, USA).

PAS staining

PAS staining is preferred for examining carbohydrate macromolecules (glycogen, glycoprotein, and proteoglycans). Basically, periodic acid breaks down two contiguous carbon bonds and produces aldehydes at the free ends. Subsequently, the Schiff reagent reacts with those aldehydes and shows a purple/magenta color. As a result of staining, positive PAS substances appear magenta red, and the nuclei appear blue.

A PAS-amylase (04-130803; Bio-Optica, Italy) staining kit was used for this experiment. Amylase is a pre-applied solution that helps obtain clear results. The kit was applied according to the manufacturer's protocol in the following steps. The slides were washed with distilled water and incubated in amylase reagent for 10 minutes at room temperature. After rinsing with distilled water, the slides were exposed to a periodic acid solution for 10 minutes. After washing in distilled water, a Schiff reagent was applied for 20 minutes. The slides were then treated with a potassium metabisulphite solution for 2 minutes after washing with distilled water. After draining the slides and soaking them in the fixative solution for 2 minutes, they were washed with distilled water. Mayer's Hemalum solution was then applied for 3 minutes and washed with tap water. Finally, the slides were dehydrated using ascending series of alcohol (70%, 96%, and 100%), cleared in xylene (1330-20-7; JT Baker, USA), and mounted. The positive PAS dots were observed by optical microscopy.

Masson's trichrome staining

Masson's trichrome staining is a common histological technique consisting of three different staining solutions. The protocol starts with Weigert's hematoxylin and continues with possible combinations of a plasma stain, a solution containing phosphomolybdic acid, and a fiber stain. Most combinations produced green or blue collagen fibers, light pink plasma, red muscle fibers, and dark brown/black nuclei.

https://doi.org/10.14405/kjvr.2021.61.e25

The slides were washed with distilled water after fixation. After Weighert's hematoxylin (05-06008A/L, 05-06008B/L; Bio-Optica) was applied for 3 minutes, the slides were washed with tap water for 10 minutes. They were then soaked in a freshly prepared acid fuchsin (F8129; Sigma-Aldrich)-phosphomolybdic acid (04-060802; Bio Optica) mixture for 5 minutes. After draining the slides, they were exposed to methyl blue (M6900; Sigma-Aldrich) for 3 minutes. They were rinsed in distilled water and treated with 1% acetic acid (1000631011; Merck KGaA, Germany) for 2 minutes. The slides were dehydrated using an ascending series of alcohol (70%, 96%, and 100%) and cleared with xylene. The slides were then mounted and observed by optical microscopy.

May-Grünwald-Giemsa staining

May-Grünwald-Giemsa staining is used mainly for blood cells. May-Grünwald contains acidic eosin, which stains the alkaline components of the cell orange/red, and alkaline methylene blue, which stains the acidic components of the cell blue. Giemsa contains azure that stains the basic cellular components red and purple.

The fixed slides were washed with distilled water and then soaked in a May-Grünwald (205435; Merck KGaA) solution for 5 minutes. After washing with distilled water, the Giemsa (48900; Sigma-Aldrich) solution was applied for 15 minutes. When the last wash was completed, the slides were left in the upright position to drain and dry. Dehydration was performed quickly in an ascending series of alcohols (70%, 96%, and 100%). The slides were cleared in xylene for 10 seconds and mounted. The morphological observations were by optical microscopy.

Diff-Quik staining

Diff-Quik is preferred for rapidly staining, which differentiates cytoplasmic elements, such as neurosecretory granules, mucins, and fat droplets in addition to nuclear staining. The slides were fixed with the first solution of the Diff-Quik (Microptic SL, Spain) staining protocol. The first solution included fast green in methanol. After dipping the slides in the fixative 5 times, slides were drained and soaked in solution 2 (Eosin G in phosphate buffer) for 2 minutes. Without washing, solution 3 (thiazine dye in phosphate buffer) was applied for 5 minutes. The slides were air-dried observed by optical microscopy without dehydrating and mounting.

Toluidine blue staining

The air-dried slides were fixed in 96% ethanol-acetone for one hour at 4°C. The preparations were hydrolyzed in 0.1 N HCl for 5 minutes and triple washed with distilled water for 2 minutes. The preparations were then stained with 0.05% toluidine blue dye (FN 1130830; Merck KGaA) for 10 minutes. After washing twice with distilled water, slides were kept in 96% alcohol for 2 minutes. The slides were then mounted and observed by optical microscopy. Pale blue nuclei were evaluated as normal, and dark blue nuclei were evaluated as chromatin destabilization.

Spermac staining

Sperm samples smeared on positively charged slides and air-dried. For acrosomal morphological examination, the Spermac stain kit (Stain Enterprise, Republic of South Africa) was used. Spermac stains the nuclear portion and the post-acrosomal region red, and the acrosome, midpiece, and tail parts of the sperm as green. The protocol was applied as Oettle [7] reported. The slides were fixed in 4% paraformaldehyde for 15 minutes and washed several times with distilled water. When the excess water was drained, the slides were placed in solution A for 1 to 2 minutes. After washing gently, the slides were soaked in solution B for 1 minute. The slides were washed with distilled water and placed into solution C for 1 minute. After the last wash, the slides were air-dried and observed by optical microscopy without mounting.

Scanning electron microscopy preparation

The collected sperm samples were spread on the positively charged slides and air-dried. The slides were fixed in a 2% paraformaldehyde-10% glutaraldehyde mixture (1:1) for 20 minutes. Subsequently, the slides were dehydrated in an increasing series of alcohol (70%, 96%, and 100%). The slides were then sputter-coated with gold/palladium particles in the Leica EM ACE200 system (Leica Microsystems GmbH, Germany) and examined using a Zeiss EVO HD 15 STEM.

Statistical analysis

SPSS for Windows ver. 16.0 software (SPSS Inc., USA) was used for statistical analysis. The mean and standard deviation of the measurements were calculated using the program.

Results

Table 1 lists detailed measurements of each part of a sperm cell shown in Fig. 1. The scheme on the left shows the images used to measure the specific area (Fig. 1). The axolotl sperm consists of an elongated head, a neck, and a flagellum covered

with an undulating membrane (Figs. 2, 3). There were no collagen fibers observed in any sperm region (Fig. 2A and B). The spermatozoa head is sickle-shaped with a tapered end as it elongate towards the tip (Figs. 2E and 3D). The scanning electron microscopy (SEM) images of the head region supported the routine optical microscopy observations (Fig. 4). The midpiece was relatively shorter and had a stable width throughout its long axis (Figs. 2E, 2F, 3A, 3B, 3E, 3F). The tail is connected to the posterior end of the neck and consists of a supporting axial rod (axial fiber) attached to a lateral flagellum by an undulating membrane (Figs. 3A, 3B, 3E, 3F, 5, and 6). The silhouette of the wavy membrane was observed with Diff-Quik staining (Fig. 3A and B) and observed clearly with Spermac staining (Fig. 3E and F). Giemsa staining showed the straight membrane pattern of the ending tail (Fig. 3C and D). The tail could be divided into a midpiece, a main piece (Fig. 3F), and an end piece (Fig. 3C, inset). The structural map of this interesting membrane was determined by SEM examinations (Figs. 5, 6). The main piece was easily discernible in *Ambystoma* because of the tail membrane [8] or keel [9] extending along it opposite the undulating membrane. The SEM images of both membranes terminated at the

Table 1. Detailed measurements

Variable	Value
Head (μm)	
Length	103.661 ± 0.6
Width (thinnest to thickest part)	0.429-1.560
Midpiece (μm)	
Length	8.575 ± 0.4
Width	1.08 ± 0.1
Tail (μm)	
Length	
Total axonem part	356.544 ± 3.1
Following undulated membrane part	300 ± 1.9
Width (undulated membrane included)	1.942 ± 0.3

Values are presented as the mean ± standard deviation unless otherwise indicated.

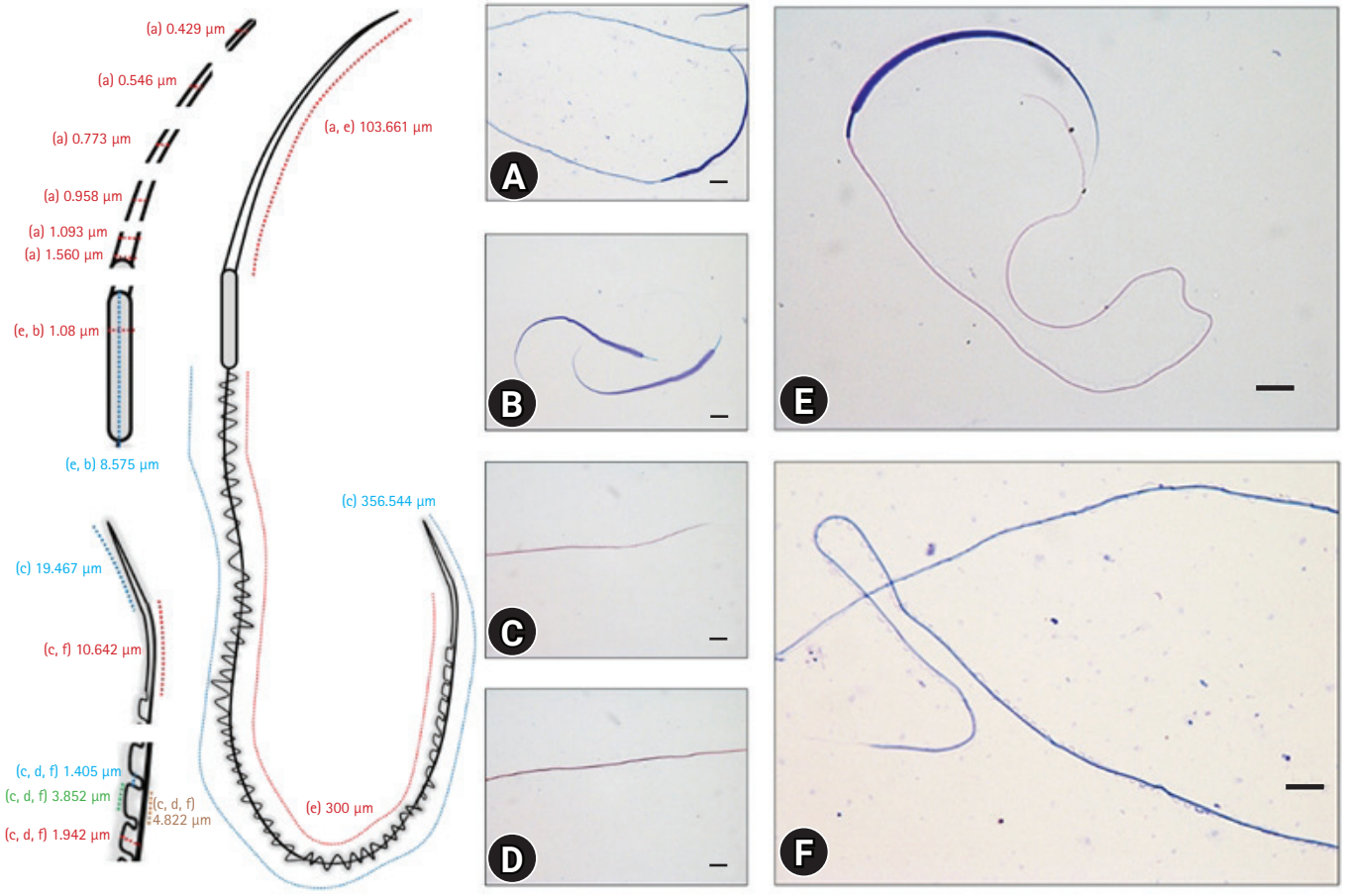

Fig. 1. Detailed measurements of a sperm cell and the measured images stained with Diff-Quik (A, E, F), toluidine blue (B), and Masson's trichrome (C, D). The scheme on the left shows the images used to measure the specific area (A and E for the head region; E and B for the midpiece region; C, D, and F for the tail region). (A-F) Scale bar: 10 μm.

https://doi.org/10.14405/kjvr.2021.61.e25

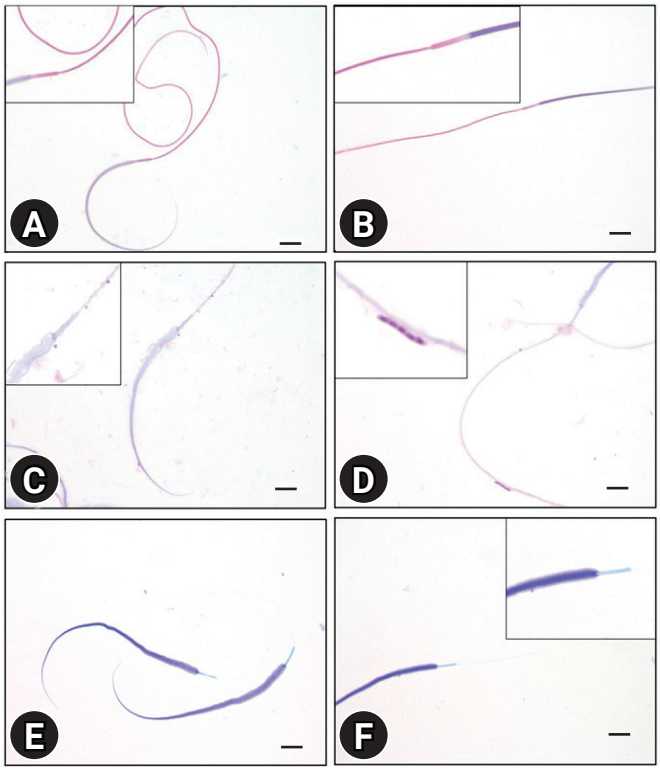

Fig. 2. No collagen fibers were observed with Masson's trichrome staining (A, B and insets); periodic acid Schiff positive granules were seen at different points of the tail and lover head (C, D and insets), and toluidine blue staining sharpened the edges of the head (E) and midpiece region (F and inset). (A-F) Scale bar: 10 μm.

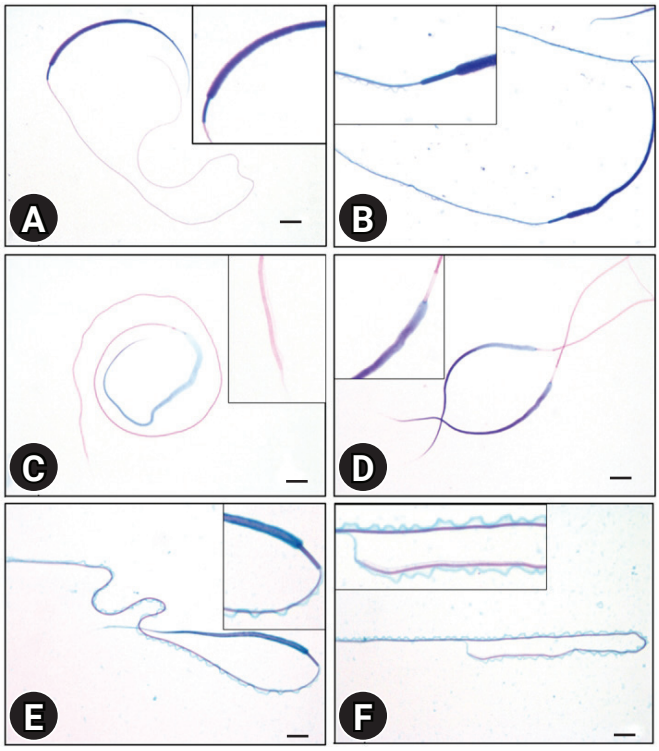

Fig. 3. Silhouette of a wavy membrane was seen with Diff-Quik staining (A, B and insets); Giemsa staining showed the straight membrane pattern of the ending tail (C, D and insets), and the wavy membrane was observed clearly by Spermac staining (E, F and insets). (A-F) Scale bar: 10 μm.

tapered end of the axial rod, but a short segment of the flagellum extended beyond the end piece. PAS-positive granules were observed clearly on the post-nuclear part of the head and tail (Fig. 2C and D). The measured length of spermatozoa was 468.78 μm.

Discussion

There is limited data on reproductive biology and gamete cells of the axolotl, which may provide insights into their regeneration potential. Regarding the morphology of axolotl sperm, only three studies have been performed, one of them focusing on the mitochondrial morphology [9]. Another focused on the testicular structure in a group of salamanders [3]. The last study examined the sperm morphological differences after interspecific hybridization [10]. Other studies included a study on semen collection strategies, with one focusing on the spermatogenesis procedure [6,10].

One study carried out in 2014 investigated the testicular structure and germ cell morphology of *A. mexicanum* [3]. The cystic structures within the testicle matured in the cephalo-caudal regions and were replaced. Spermatogonial stem cells were observed in the cystic structures in the cephalic region of the testis, and mature spermatids were noted in the cystic structures in the caudal region. Uribe and Mejía-Roa [3] reported the morphology of the axolotl sperm in general with hematoxylin-eosin staining. The mature spermatozoa contained acrosomes and nuclei in the head. During maturation, the nucleus of the sperm is elongated and acquires a sickle appearance. The neck (middle part) part is rich in mitochondria, providing energy for movement. In the flagellum (tail) part, the wavy membrane structure, whose function has not been explained, surrounds the tail [3].

The axolotl sperm was demonstrated with different staining methods, and a detailed measurement was performed for each region for the first time. The results represent the mean value (average) taken from three axolotls to exclude the slight variations among spermatozoa from a single male. The overall sperm length was 468.78 μm, which is different from the 444 μm reported by Uribe and Mejía-Roa [3]. This difference may-

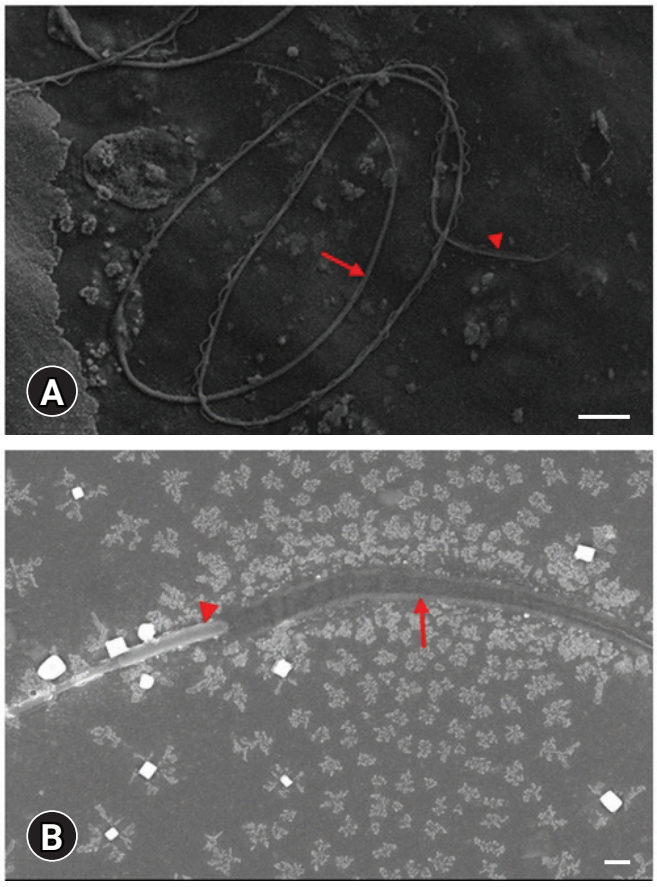

Fig. 4. Scanning electron microscopy images. (A) Whole sperm cell. The red arrow indicates the head part, and the arrowhead indicates the last straight membrane part of the tail. (B) The red arrow indicates the head, and the arrowhead indicates the midpiece structures of a sperm cell. Scale bar: (A) 10 μm, (B) 2 μm.

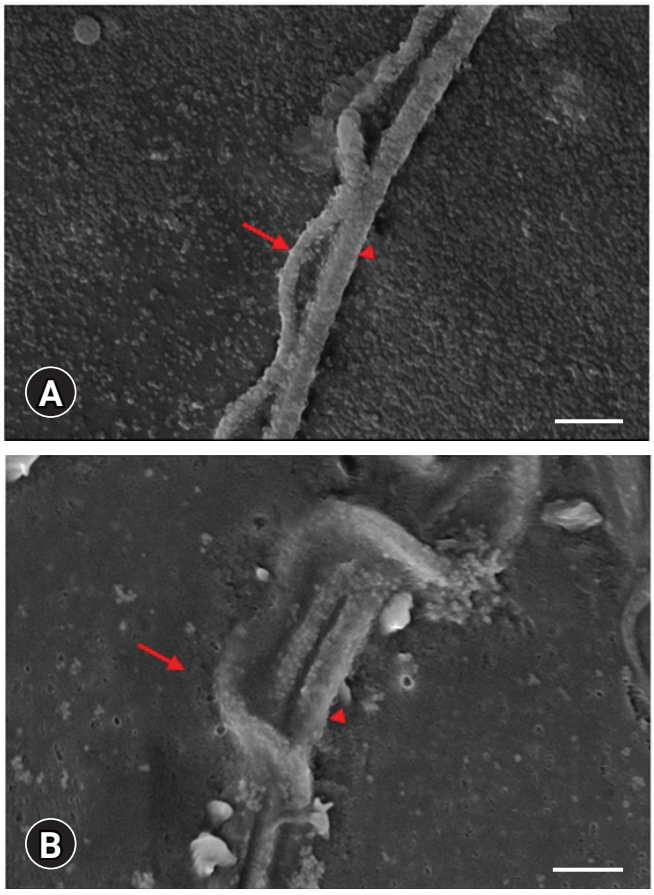

Fig. 5. Scanning electron microscopy images. Undulated membrane (arrow) and tail (arrowhead) structures of sperm cells. Scale bar: (A) 2 μm, (B) 1 μm.

be because of the different stocks used in the studies.

PAS-positive granules were observed clearly on the tail, indicating the cellular transport of a sperm cell. Axolotl sperm cells move forward circularly. These energy-containing packages might contribute to the tail movement. The other important question is the direction of these granules, which could provide information on the sperm cell metabolism. Further detailed research will be necessary to understand this model organism better.

No abnormal sperm cells were observed in any of the individuals. Uribe and Mejía-Roa [3] reported some abnormally sized and shaped spermatozoa in several cysts. Spermatozoa mature in the cystic structures in the axolotl testicular lobules. They also reported that these spermatozoa were eventually phagocytized by Sertoli cells, which is in accordance with the present findings. Overall, all the abnormal sperm cells were phagocytized, resulting in no abnormal sperm cells remaining, unlike humans. This is a notable finding regarding the high regeneration capacity of the axolotl. The results suggest that the molecular mechanisms underlying the high regeneration capacity may explain the elimination of abnormal forms. The detailed morphologic analysis of the axolotl sperm was carried out using different staining methods, which require further analyses with special insight into molecular events and the mechanisms used to eliminate the abnormal sperm cells. This may provide clues to understand the mechanisms underlying male factor infertility correlated with sperm parameters and develop treatment strategies by propagating the elimination mechanisms to prevent infertility.

Acknowledgments

The authors thank Ali Şenbahçe for helping animal care of the manuscript.

https://doi.org/10.14405/kjvr.2021.61.e25

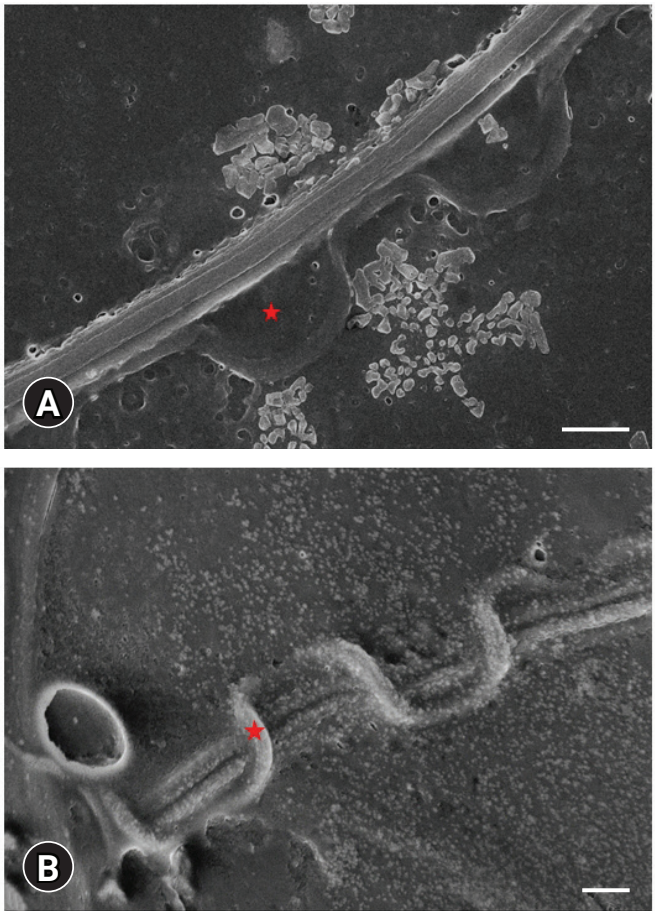

Fig. 6. Scanning electron microscopy images. Undulated membrane (indicated as a red star) and tail structures of sperm cells. (A, B) Scale bar: 1 μm.

ORCID

İlknur Keskin, https://orcid.org/0000-0002-7059-1884
Duygu Gürsoy Gürgen, https://orcid.org/0000-0001-6698-9032
Didem Avinca, https://orcid.org/0000-0001-9724-6733
Ekrem Musa Özdemir, https://orcid.org/0000-0001-9416-7757
Suat Utku Keskin, https://orcid.org/0000-0002-2277-3800
Seda Karabulut, https://orcid.org/0000-0003-3302-5004

References

1. Tanaka EM, Reddien PW. The cellular basis for animal regeneration. Dev Cell 2011;21:172–185.
2. Joven A, Elewa A, Simon A. Model systems for regeneration: salamanders. Development 2019;146:dev167700.
3. Uribe MC, Mejía-Roa V. Testicular structure and germ cells morphology in salamanders. Spermatogenesis 2015;4:e988090.
4. Sever DM. Female sperm storage in amphibians. J Exp Zool 2002;292:165–179.
5. Watanabe A, Onitake K. The urodele egg-coat as the apparatus adapted for the internal fertilization. Zoolog Sci 2002;19:1341–1347.
6. Mansour N, Lahnsteiner F, Patzner RA. Collection of gametes from live axolotl, Ambystoma mexicanum, and standardization of in vitro fertilization. Theriogenology 2011;75:354–361.
7. Oettle EE. Using a new acrosome stain to evaluate sperm morphology. Vet Med 1987;81:263–266.
8. Martan J, Wortham E. A tail membrane on the spermatozoa of some ambystomatid salamanders. Anat Rec 1972;172:460.
9. Noblb GK, Brady MK. Observations on the life history of the marbled salamander, Ambystoma opacum gravenhorst. Zoologica 1933;11:89–132.
10. Miltner MJ, Armstrong JB. Spermatogenesis in the Mexican axolotl, Ambystoma mexicanum. J Exp Zool 1983;227:255–263.